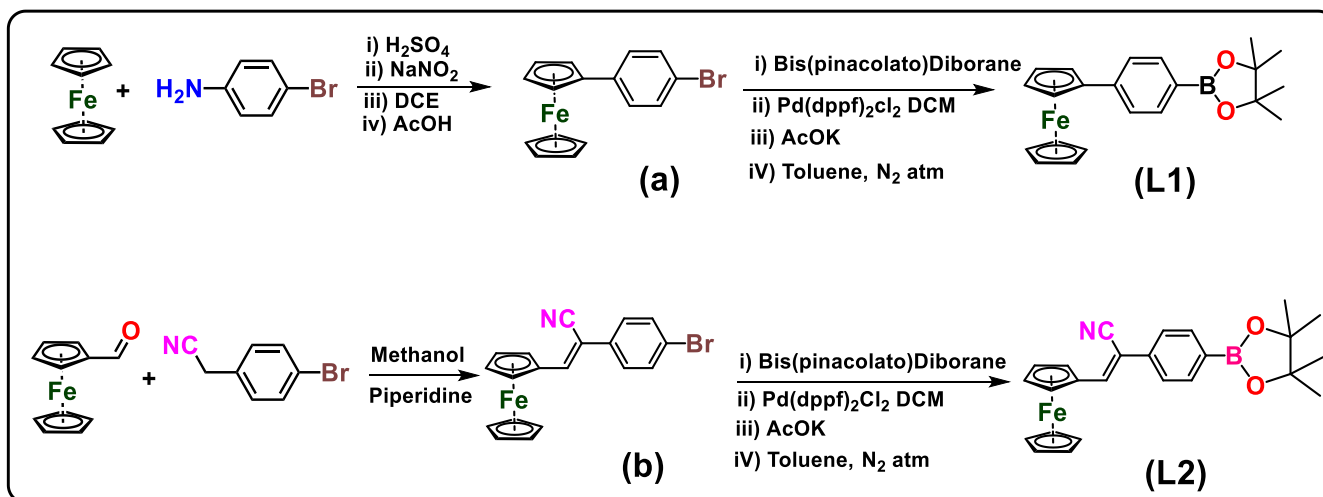


Ferrocene-Appended Boronated Ester: Effect of Cyanovinylene Group on the Nonlinear Optical Properties and Colorimetric Detection of Fluoride ion

Thamodharan Viswanathan^a and Nallasamy Palanisami^{a*}

^aCenter for Functional Materials, Department of Chemistry, School of Advanced Sciences, Vellore Institute of Technology, Vellore - 632014, Tamil Nadu, India.

*Corresponding Author: Email: palanisami.n@gmail.com; Tel: +91 9842639776.



Scheme S1 Synthesis of receptors **L1** and **L2**.

Cyclic voltammetry (CV)

$$E_{1/2} = (E_{pa} + E_{pc})/2 \dots \dots \dots (1)$$

$$\Delta E = E_{pa} - E_{pc} \dots \dots \dots (2)$$

Where, anodic peak potential (E_a), anode current (i_a), cathodic peak potential (E_c), cathode current (i_c), the half-wave potential ($E_{1/2}$) and peak separation (ΔE).¹

Solution Preparation for sensing of F^- ion

The stock solution of ligand (10 ml) and various anions (10 ml) were prepared at the concentration of 1×10^{-3} M using chloroform solvent. Further, the ligand solution 1×10^{-6} M (10 ml) was prepared from the stock solution by serial dilution, and also anions were diluted into 1×10^{-4} M (10 ml). These solutions were directly used for the UV-Visible and fluorescence titrations. The fluorescence maxima of **L2** at 375 nm were observed with the excitation of 295 nm.

Detection limit

The detection limit was calculated based on the fluorescence titration. The emission spectrum of ferrocenyl boronated ester **2** as a function of its increasing concentration was measured five times, and the standard deviation of blank measurement was achieved. To gain the slope, the ratio of emission intensity at 372 nm in chloroform solution was plotted against the concentration of F^- ion. The detection limit was calculated using the following equation,²

$$Detection\ Limit = 3\sigma/K$$

Where, σ is the standard deviation of blank measurement, and K = slope of the plot between the ratio of emission intensity versus F^- ions.

NLO Measurements (SHG)

The SHG efficiency of receptors **L1** and **L2** were studied by the Kurtz and Perry powder technique using Nd:YAG laser with a fundamental wavelength of 1064 nm.³ Grinded samples with a particle size of 80 μm were taken in a glass capillary tube and secured with tape of 1 mm thick and aluminum holders containing an 8 mm diameter hole, and potassium dihydrogen phosphate (KDP) was taken as a reference material for the measurement. A Quanta-Ray spectra physics Nd:YAG laser-producing pulses with a width of 8 ns and a repetition rate of 10 Hz were used in this study. The laser beam was passed through an IR reflector and then directed to the sample holder. The incident optical signal in PMT was converted into voltage output at the CRO (Tektronix TDS 305213)

Electrophilicity Index of Lewis Sites

The electrophilicity index is computed by following equation,⁴⁻⁵

$$\omega = \mu^2/2\eta \dots \dots \dots (3)$$

Where, μ and η are the chemical potential and chemical hardness, respectively,⁶

$$\mu = (\text{LUMO} + \text{HOMO}) / 2 \text{ and } \eta = (\text{LUMO} - \text{HOMO}) / 2$$

Where, LUMO is the energy of the lowest unoccupied molecular orbital and HOMO is the energy of the highest occupied molecular orbital.

Polarizability and Hyperpolarizability

The molecular polarizability of the receptors depends on the efficiency of electronic communication between donor and acceptor groups, playing a key role in determining the intra-molecular charge transfer. The polarizability and first hyperpolarizabilities of **L1** and **L2** were computed using DFT/B3LYP/6-31+G** level of theory. The values of the first hyperpolarizability (β), dipole moment (μ) and polarizability (α) of receptors were reported in the atomic mass units (a.u) and electrostatic unit (esu). The first hyperpolarizability is a third rank tensor that can be described by $3 \times 3 \times 3$ matrix. The components of β are defined as the

coefficients in the Taylor series expansion of the energy in the external electric field. When the external electric field is weak and homogeneous, this expansion becomes

$$E = E^0 - \mu_\alpha F_\alpha - 1/2 \alpha_{\alpha\beta} F_\alpha F_\beta - 1/6 \beta_\alpha \beta_\gamma F_\alpha F_\beta F_\gamma + \dots \quad (4)$$

Where, E^0 is the energy of the unperturbed molecules, F_α is the field at the rigid, μ_α , $\alpha_{\alpha\beta}$ and $\beta_{\alpha\beta\gamma}$ are the components of dipole moment, polarizability and the first order hyperpolarizabilities respectively. For calculating the magnitude of total static dipole moment (μ_{tot}), the mean polarizability (α_0) and the mean first hyperpolarizability (β_0) are followed as given in the literature.⁷⁻⁸ The mean polarizability defined by the following equation,

$$\alpha_0 = (\alpha_{xx} + \alpha_{yy} + \alpha_{zz})/3 \dots \quad (5)$$

The components of the first hyperpolarizability can be calculated using the following equation,

$$\beta_0 = (\beta_x^2 + \beta_y^2 + \beta_z^2)^{1/2} \dots \quad (6)$$

Where, $\beta_x = \beta_{xxx} + \beta_{yyy} + \beta_{zzz}$; $\beta_y = \beta_{yyy} + \beta_{yzz} + \beta_{yxx}$; $\beta_z = \beta_{zzz} + \beta_{zxx} + \beta_{zyy}$ is the complete equation for calculating the magnitude of β_0 . The total dipole moment can be calculated using the following equation.

$$\mu_t = (\mu_x^2 + \mu_y^2 + \mu_z^2)^{1/2} \dots \quad (7)$$

Electrophilicity index, Polarizability and hyperpolarizability

The electrophilicity index (ω) values were calculated using the reported equations (ESI)⁹⁻¹¹ and the electric dipole moment (μ_{tot}), polarizability (α_0) and hyperpolarizability (β_0) were obtained by B3LYP/6-31+G** level of theory and the values were listed in Table S8. The computed nonlinear optical (NLO) parameters like μ_{tot} , α_0 , and β_0 of the molecules depend on the electronic communication or charge separation between the donor and acceptor chromophores through π -bridge (D- π -A), which is a key role.¹²⁻¹⁴ The calculated NLO parameters μ_{tot} , α_0 , and β_0 of receptor **L2** is higher than **L1**, because, strong electron-withdrawing cyanovinylene unit is present in **L2**. Also, **L2-F** have higher μ_{tot} , α_0 , and β_0 values than receptors **L1** and **L2**, due to the influence of fluoride ion (B-F bond formation). The calculated NLO parameters such as μ_{tot} , α_0 , and β_0 using B3LYP/6-31+G** level of theory were

compared with experimental results, obtained by Kurtz and Perry powder method. The receptor **L2** shows enhanced NLO efficiency than **L1**, this is attributed to the presence of a strong electron-withdrawing cyanovinylene group.

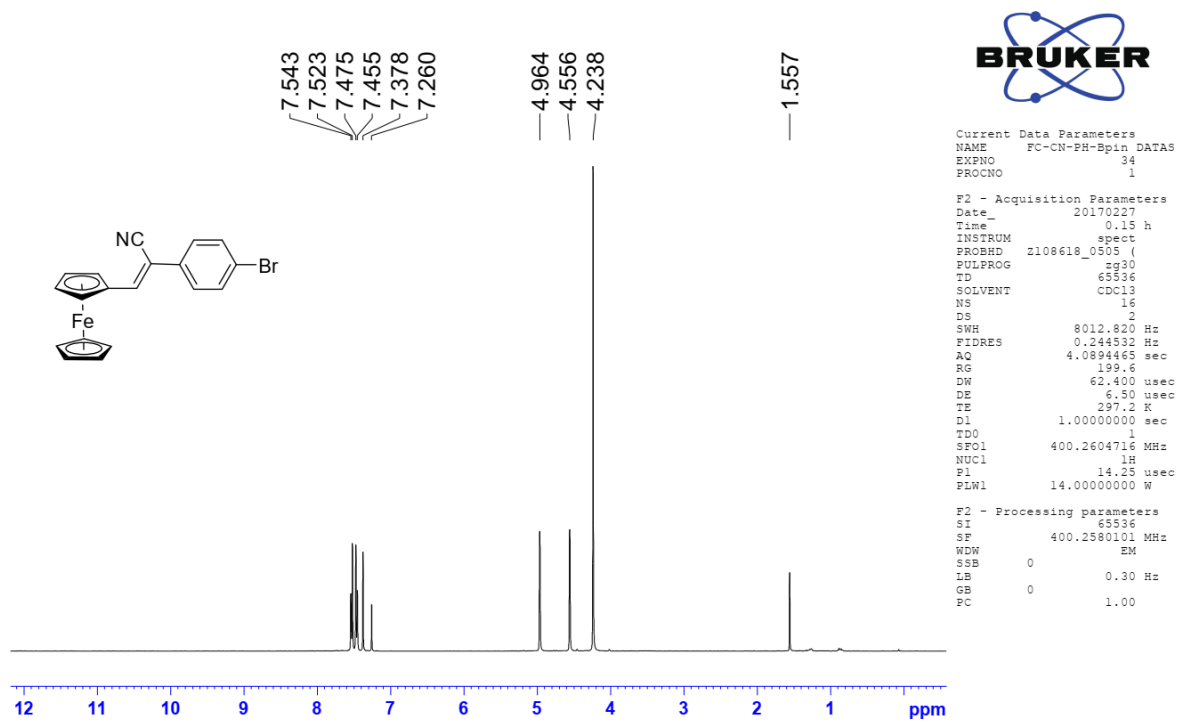


Fig. S1 ^1H NMR spectrum of 4-Bromophenylacetonitrile ferrocene (**b**) in CDCl_3 .

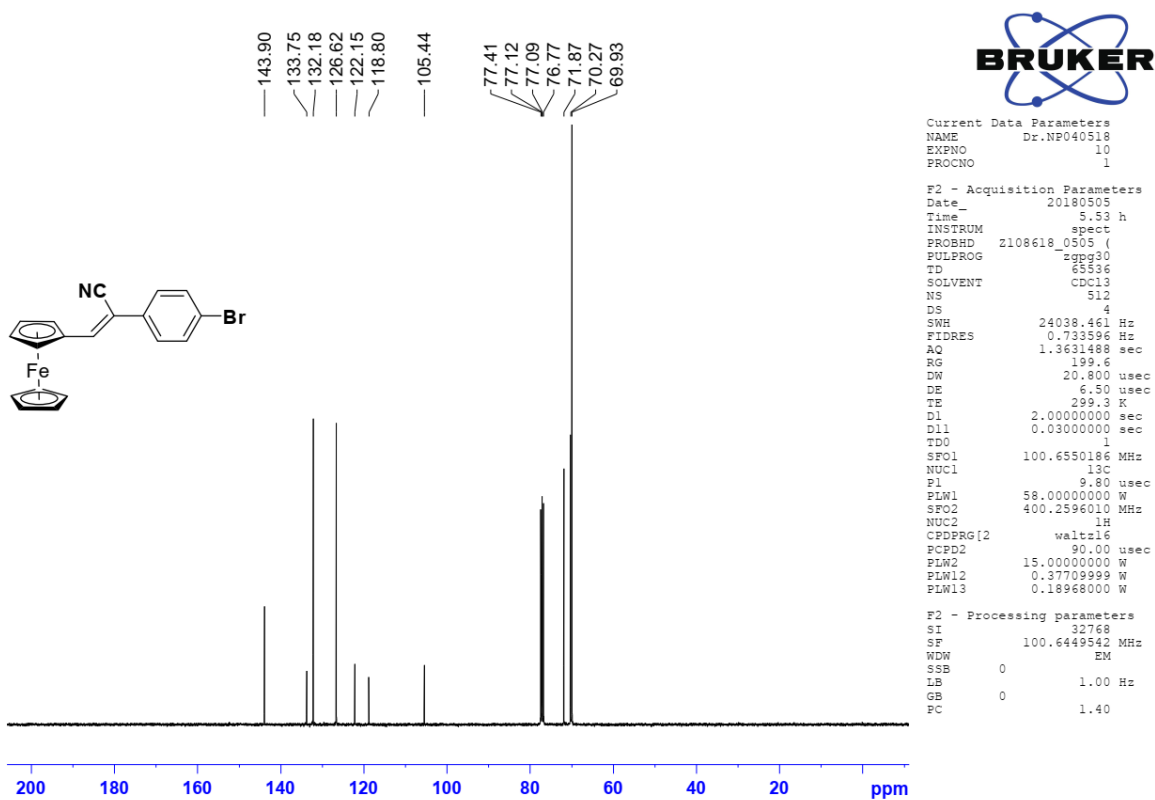


Fig. S2 ^{13}C NMR spectrum of 4-Bromophenylacetonitrile ferrocene (**b**) in CDCl_3 .

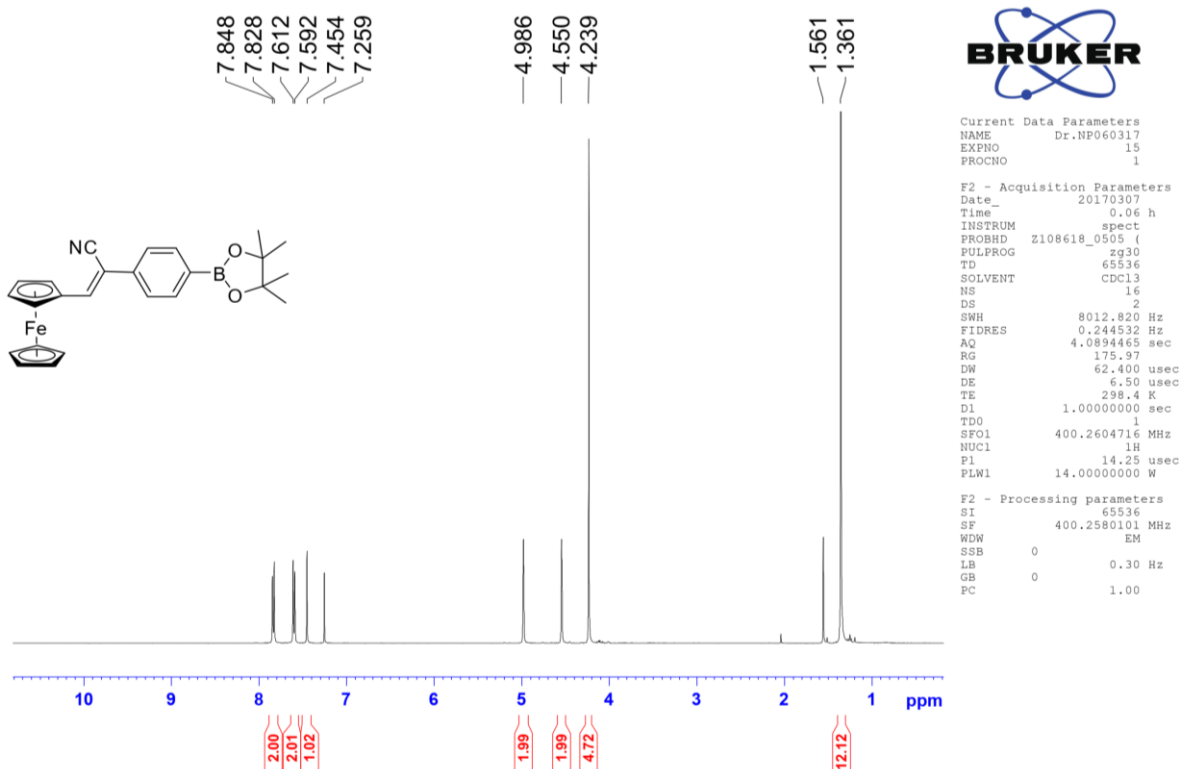


Fig. S3 ^1H NMR spectrum of receptor **L2** in CDCl_3 .

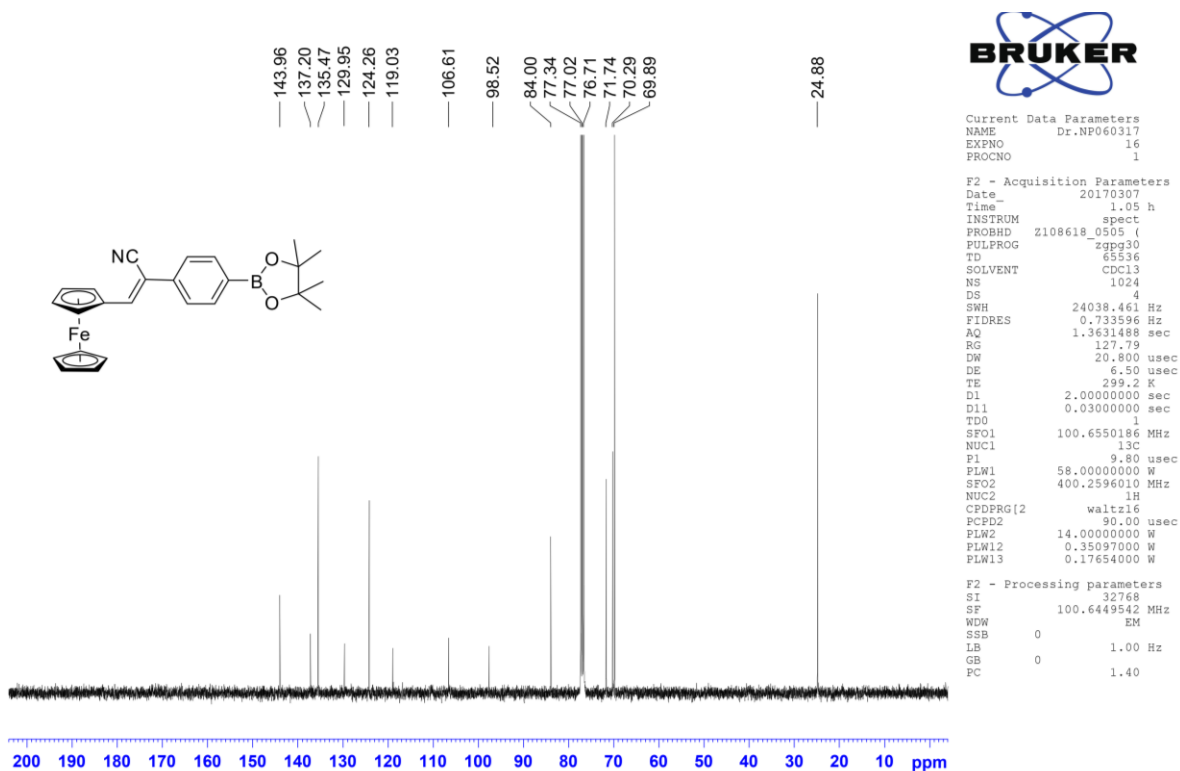


Fig. S4 ^{13}C NMR spectrum of receptor **L2** in CDCl_3 .

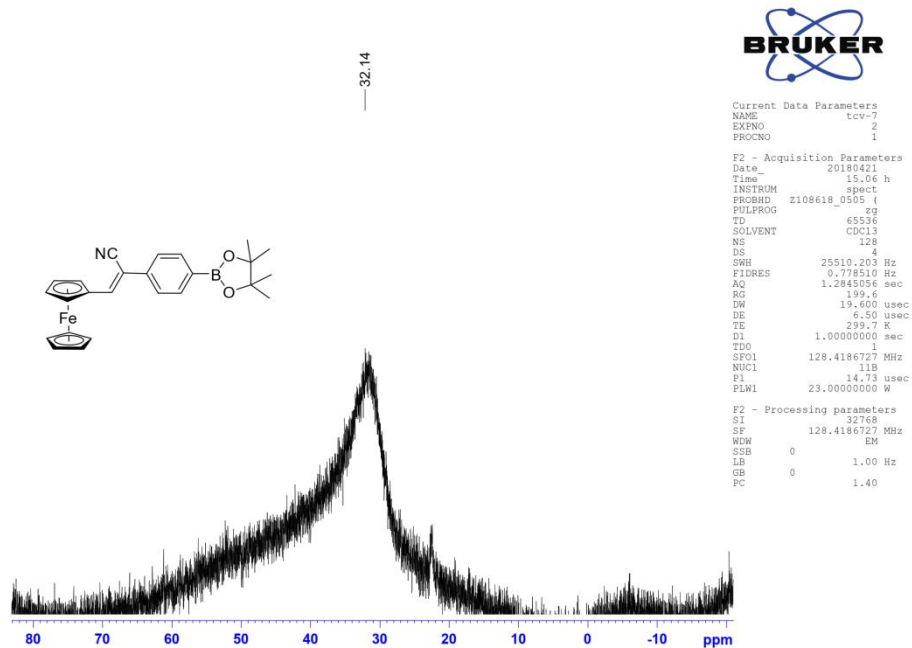


Fig. S5 ^{11}B NMR spectrum of receptor **L2** in CDCl_3 .

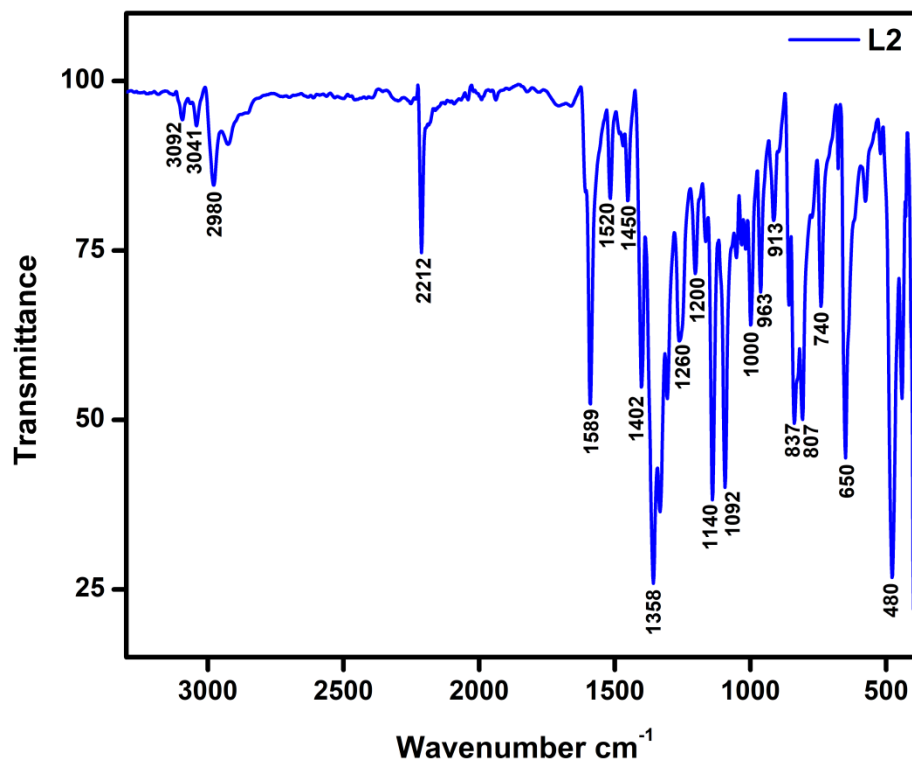


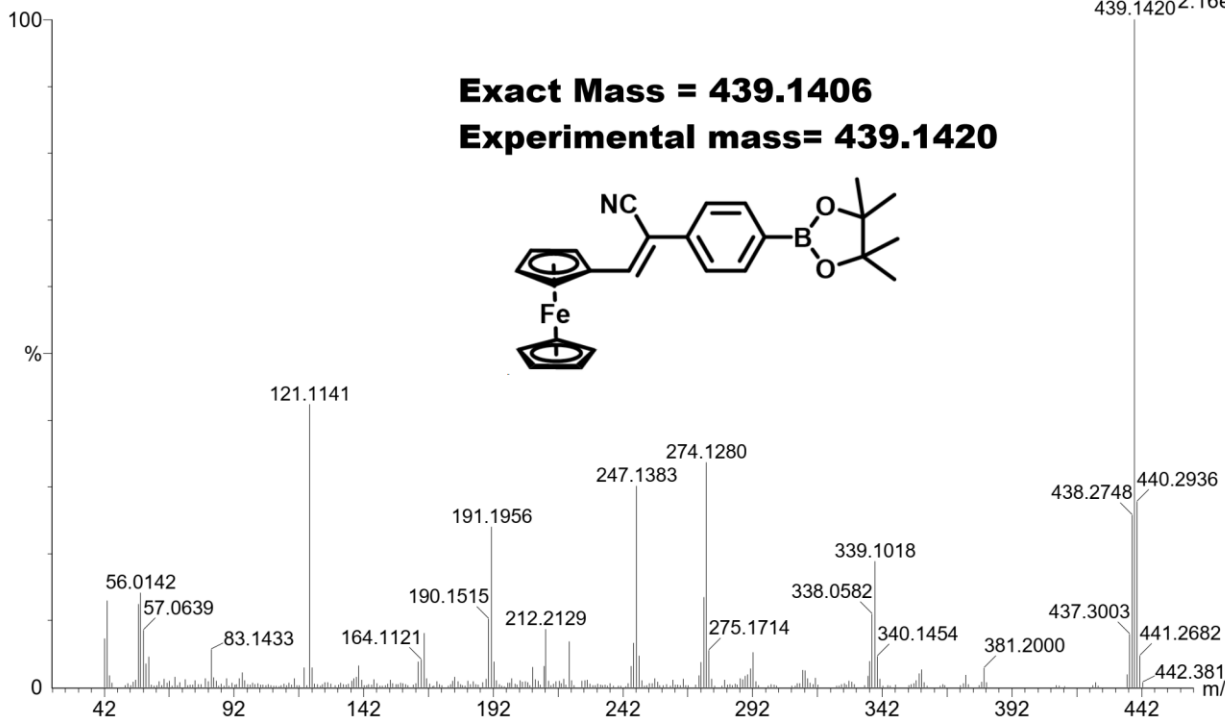
Fig. S6 FT-IR spectrum of receptor **L2** in CDCl_3 .

, 02-Mar-2017 + 22:18:58

tcv-7-(17is-0477) 5566 (30.639)

Scan EI+

439.1420^{2.16e8}



tcv-7-(17is-0477)

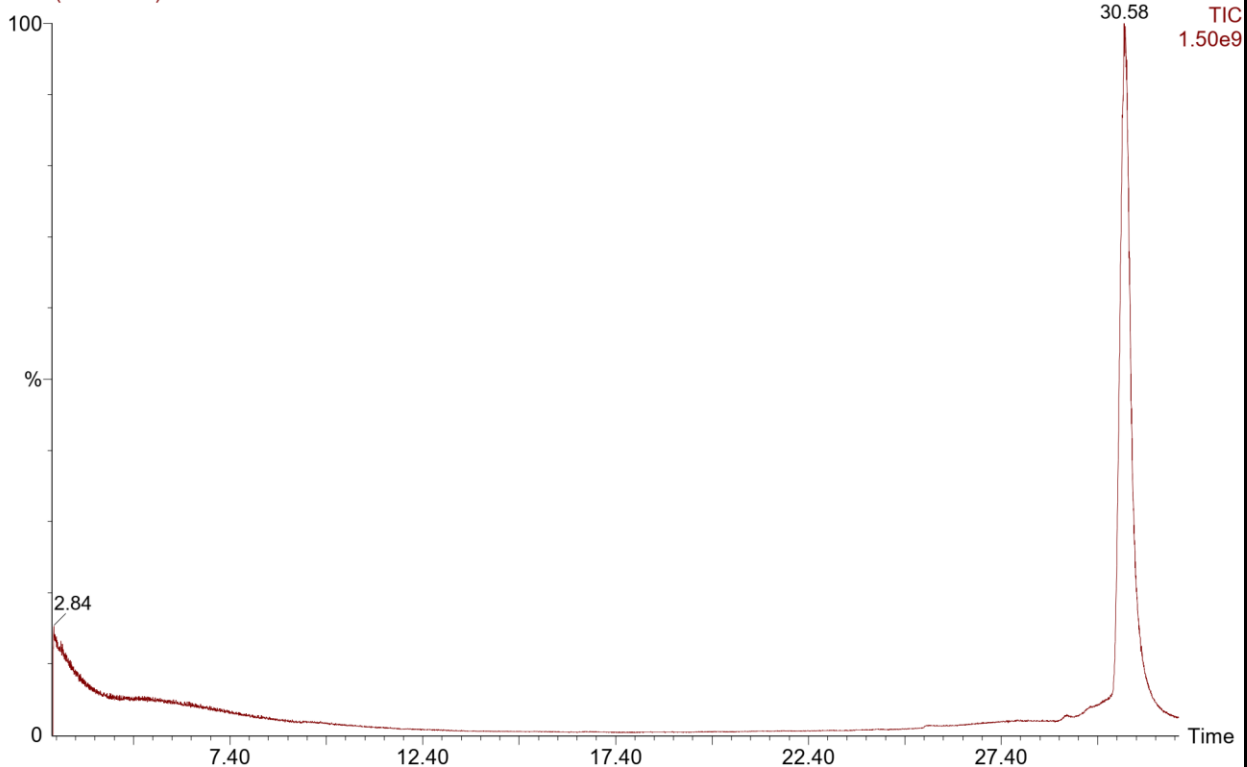


Fig. S7 GC-MS spectrum of receptor L2.

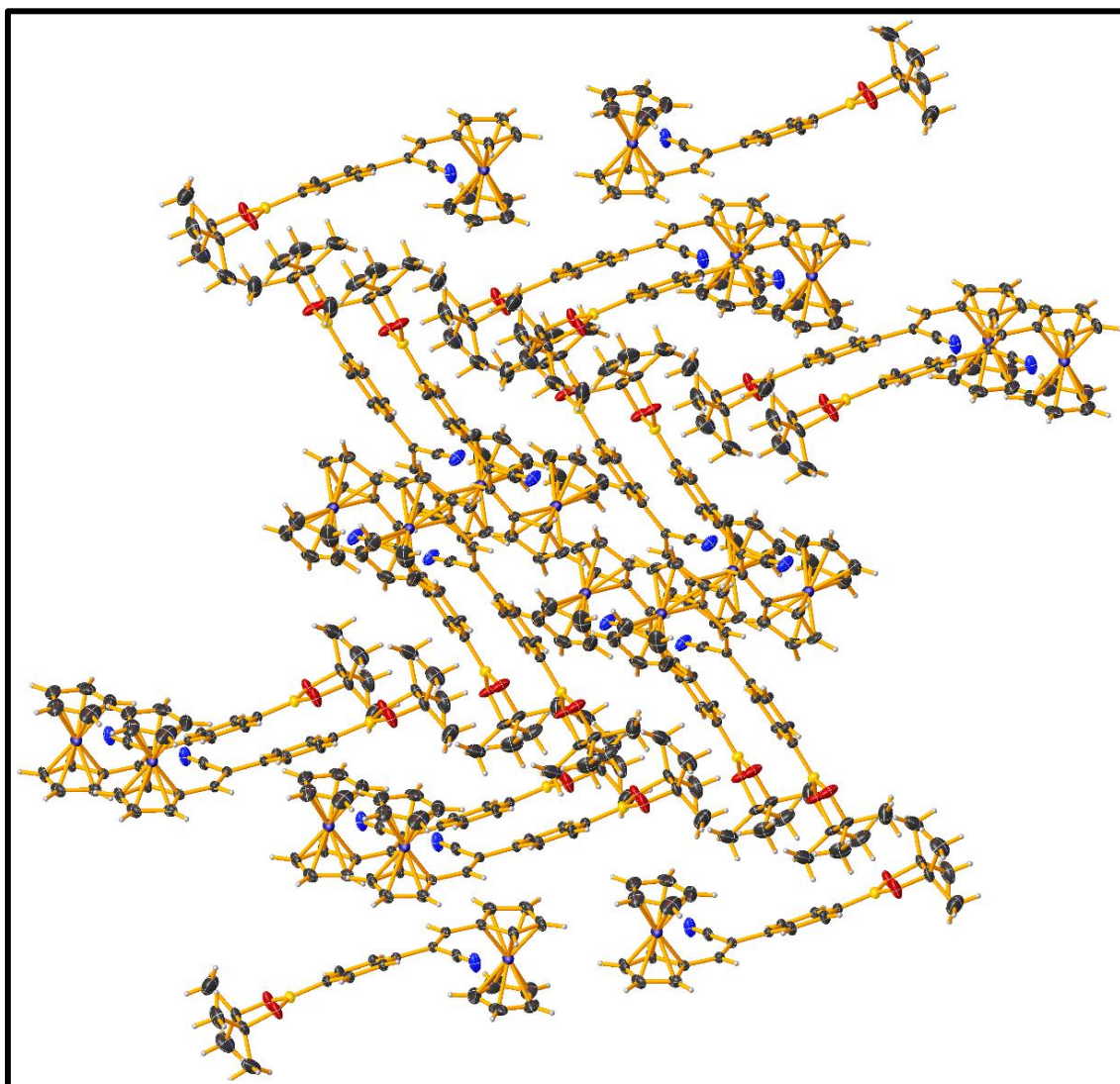


Fig. S8 Antiparallel arrangement of receptor **L2** in crystal packing.

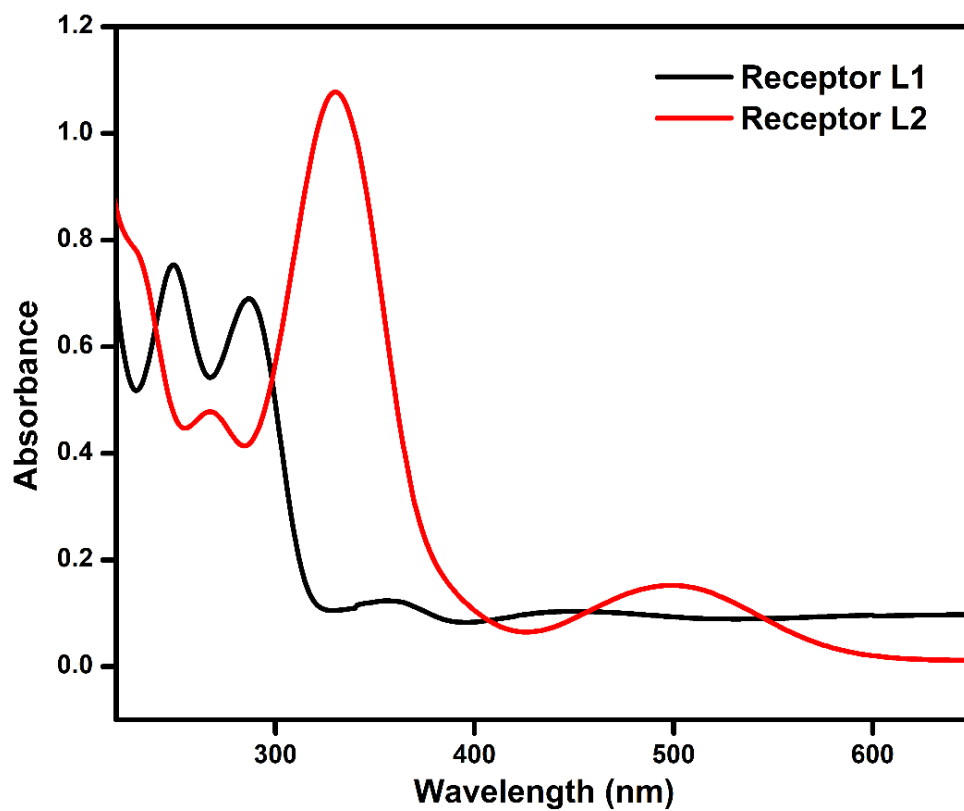


Fig. S9 UV-Visible absorption spectra of receptors L1 and L2 in chloroform solution (1×10^{-6}).

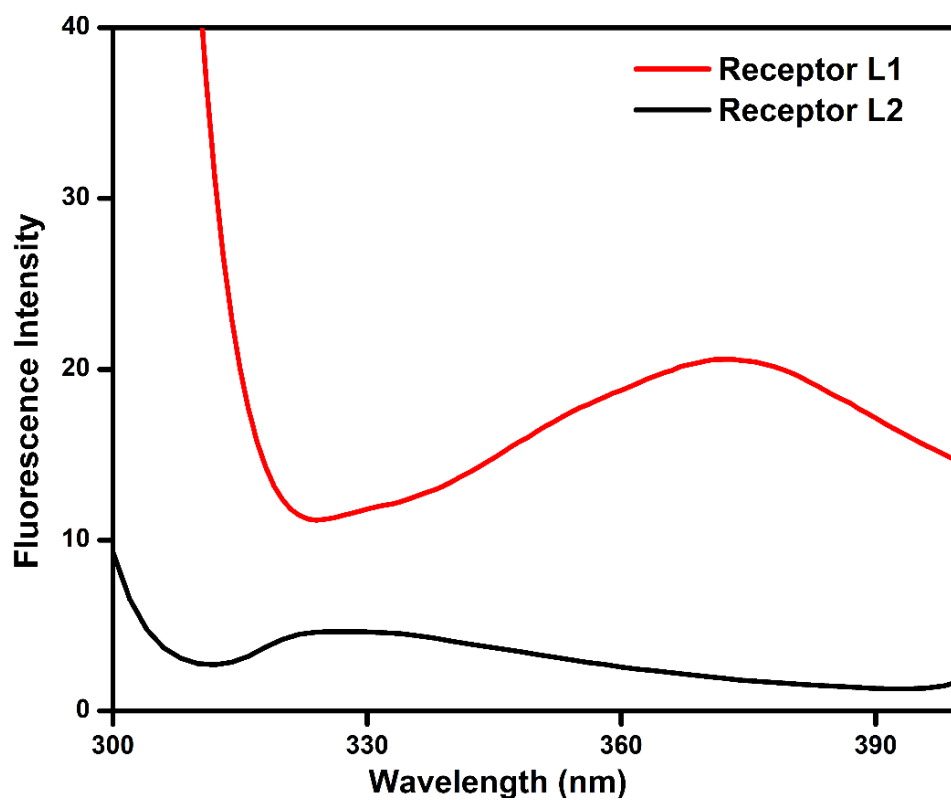


Fig. S10 Emission spectra of receptors L1 and L2 in chloroform solution (1×10^{-6}).

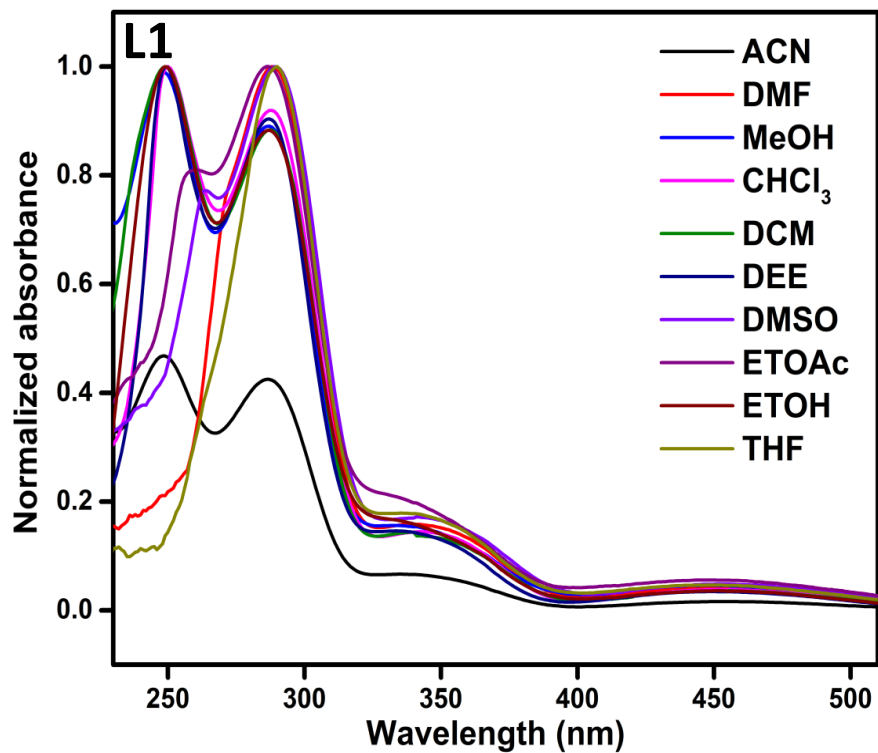


Fig. S11 UV-Visible absorption spectra of the receptor **L1** in various polarity of the solvents (1×10^{-6}).

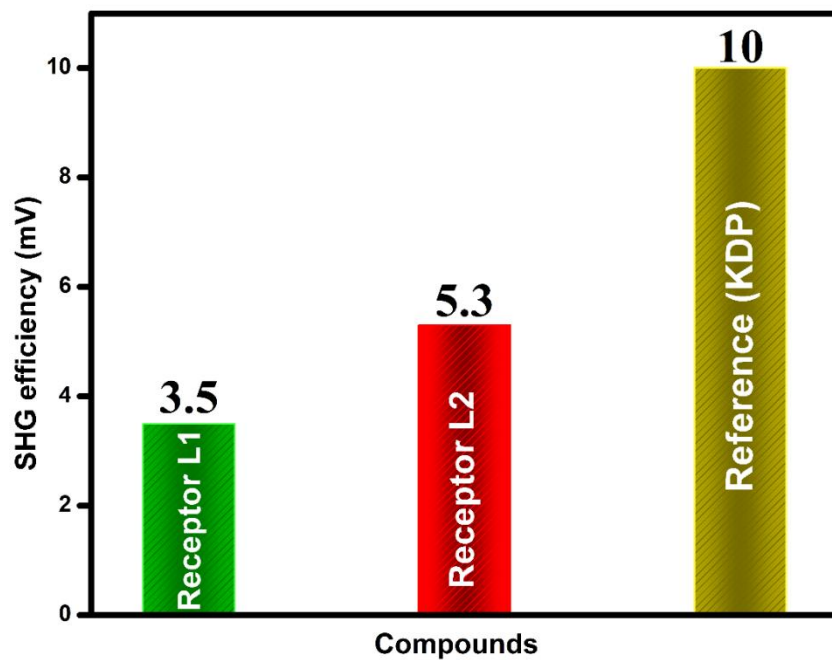


Fig. S12 SHG-NLO efficiency of receptors **L1** and **L2** by Kurtz and Perry powder method.

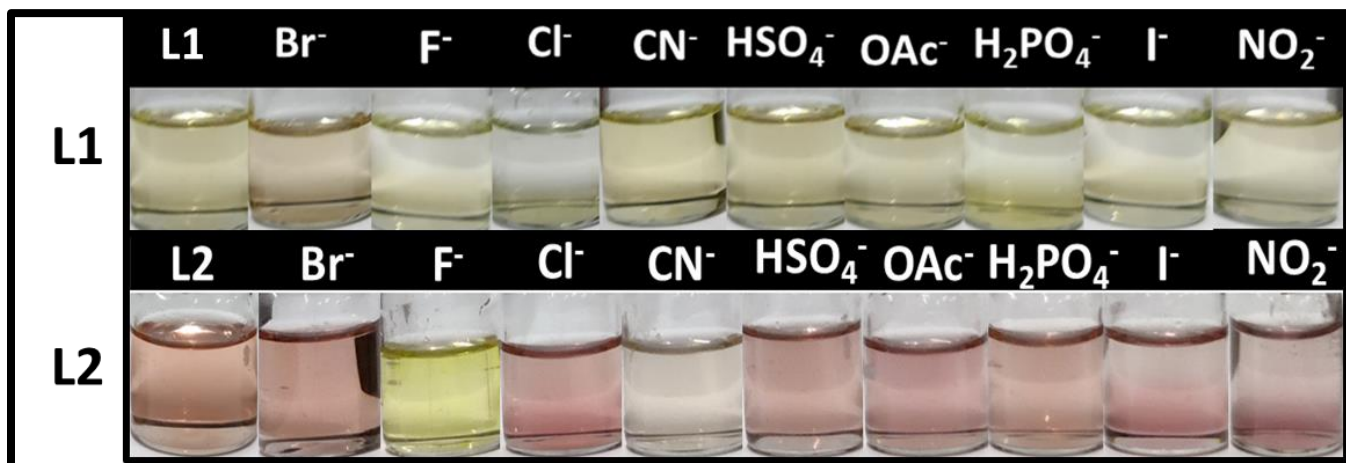


Fig. S13 Naked-eye detection of receptors **L1** (a) and **L2** (b) in chloroform solution with various tetrabutylammonium salts.

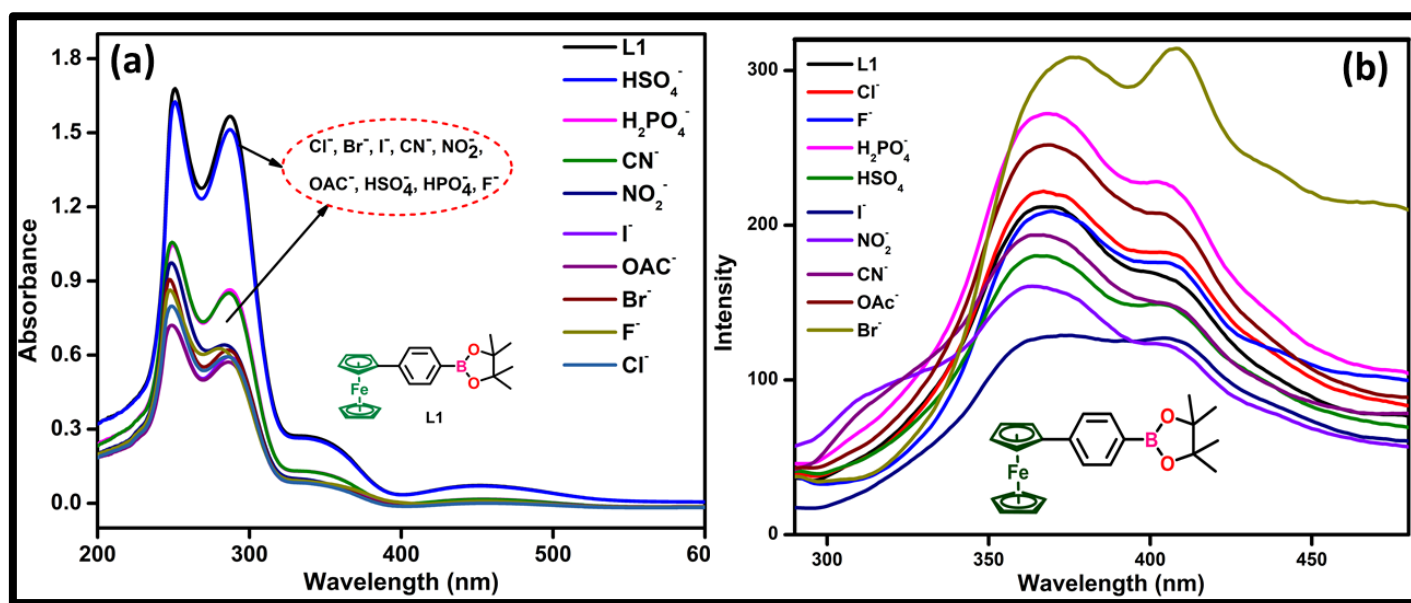


Fig. S14 Selectivity of **L1** (1×10^{-6} M) with various tetrabutylammonium salts (1×10^{-4} M) in chloroform solution using UV- visible (a) and Fluorescence (b).

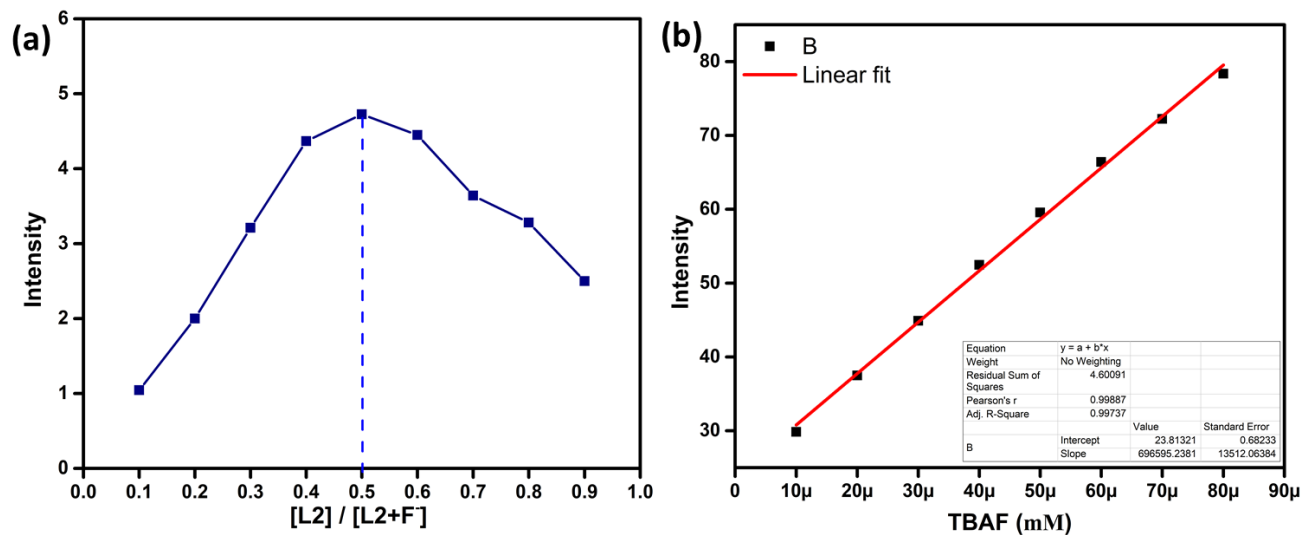


Fig. S15 Job's plot of L2 with F^- ions, demonstrates the formation of 1:1 complexation (a), the limit of detection plot (LOD) (b).

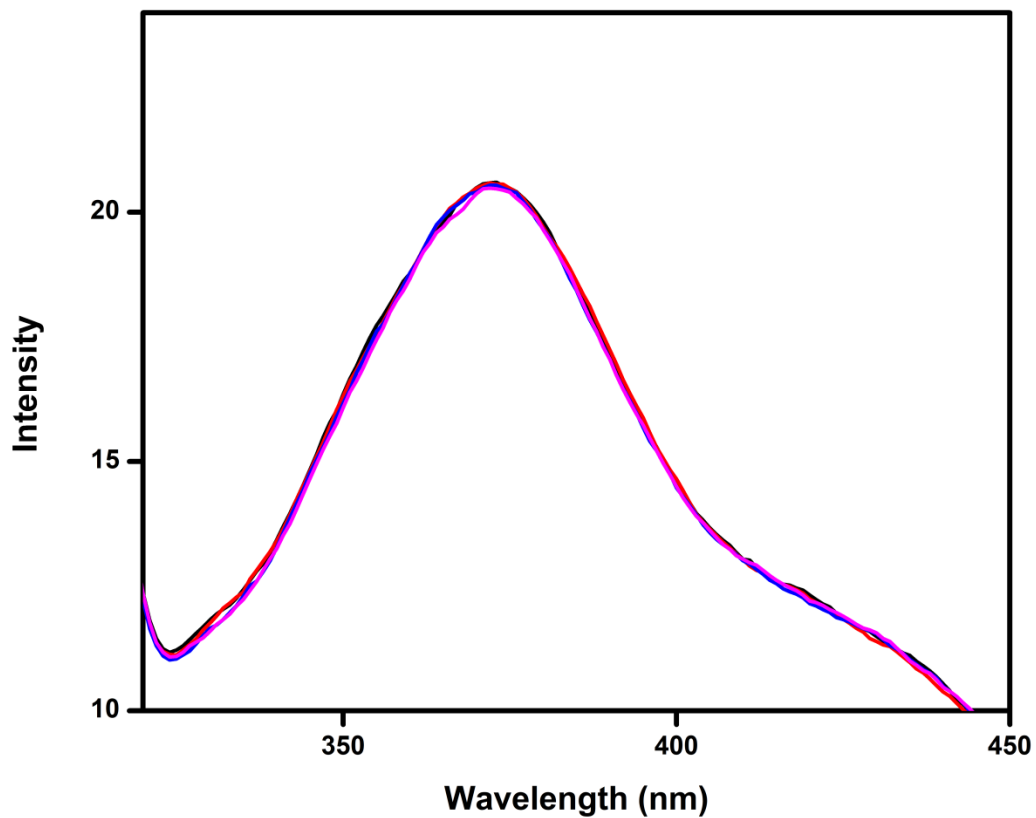


Fig. S16 The standard deviation of blank measurement (1×10^{-6}) of receptor L2.

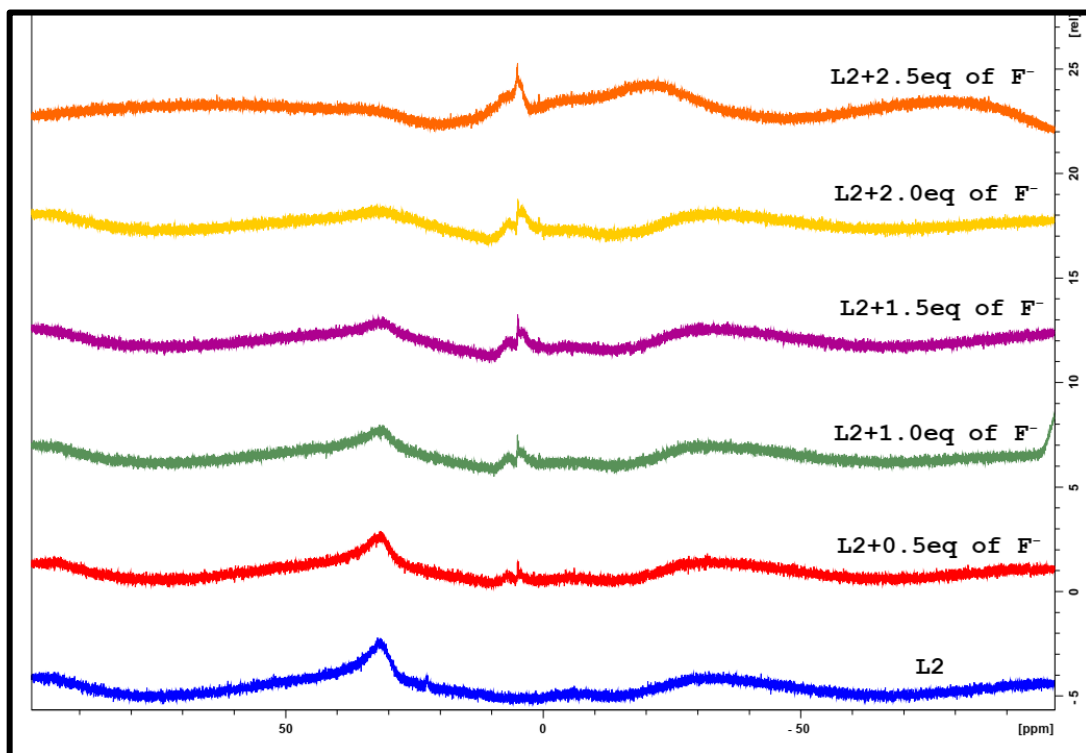


Fig. S17 ^{11}B NMR spectra of receptor **L2** (1×10^{-3} M) in CDCl_3 upon the addition of various concentrations of F^- ion.

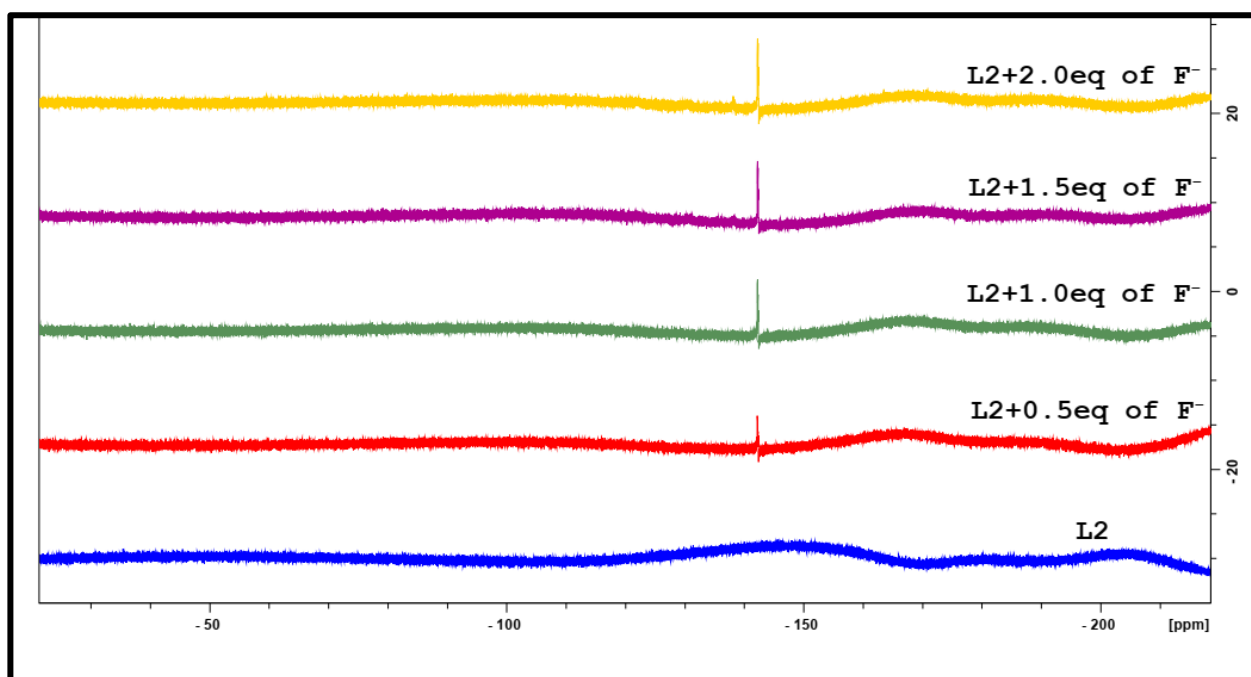


Fig. S18 ^{19}F NMR spectra of receptor **L2** (2×10^{-3} M) in CDCl_3 upon the addition of various concentrations of F^- ion.

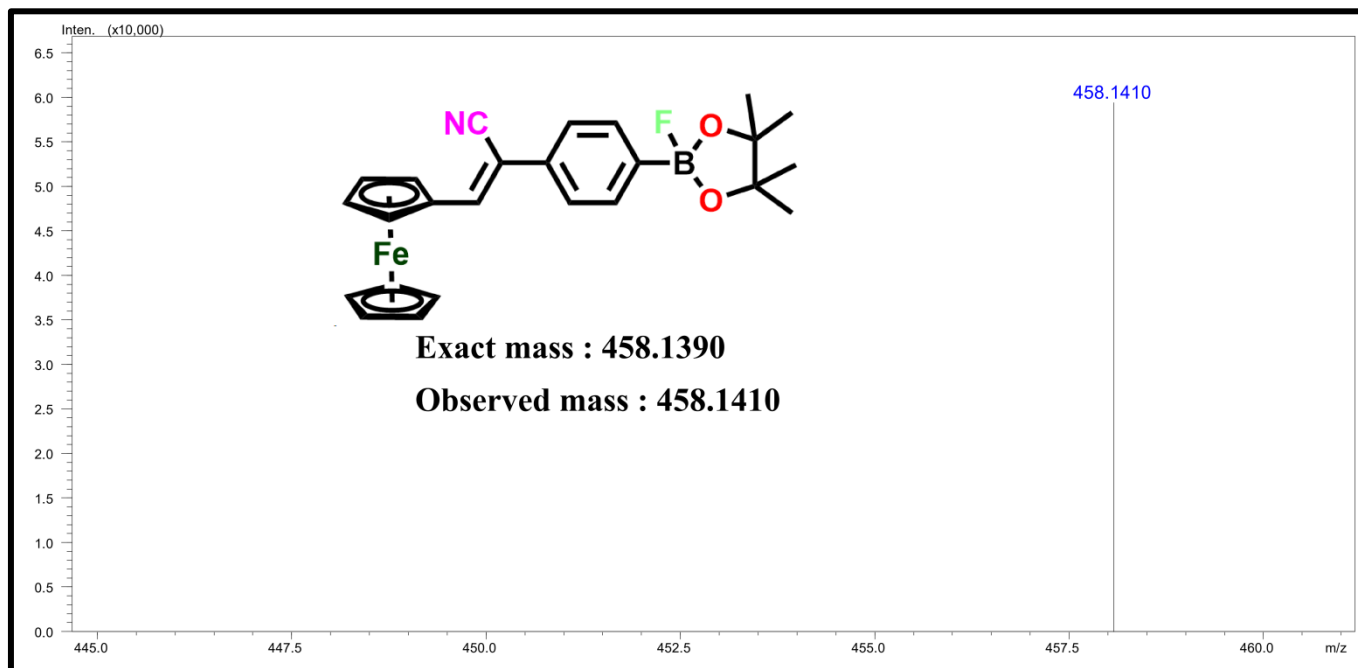


Fig. S19 ESI-Mass Spectrum of complex **L2+F⁻**.

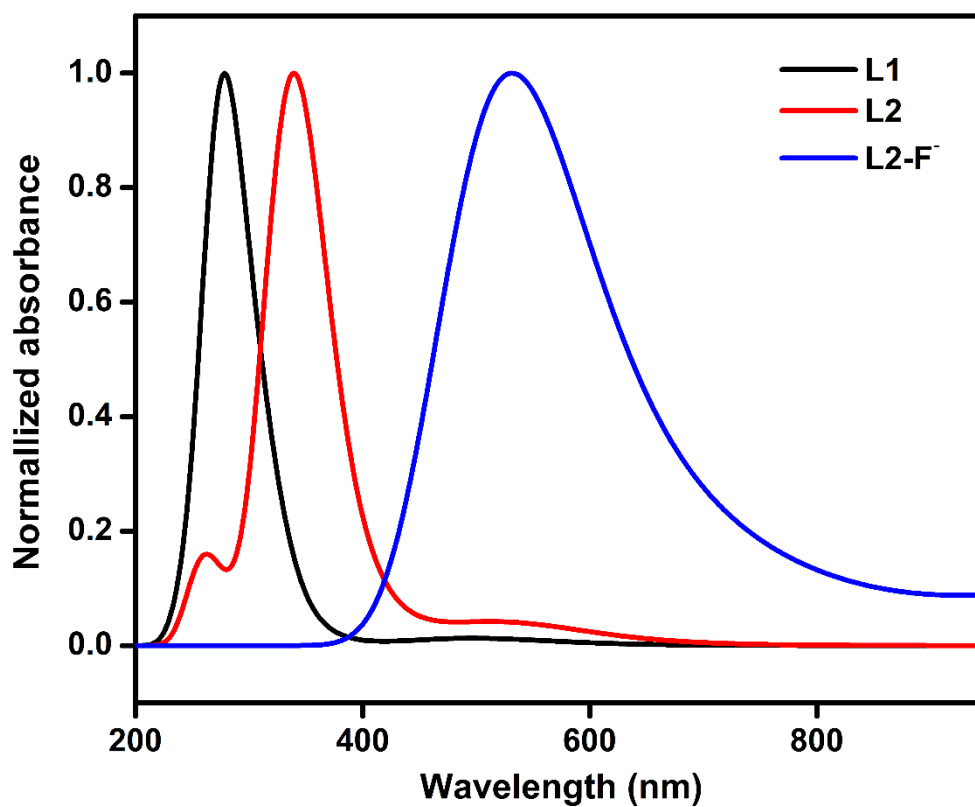


Fig. S20 Computed UV-Visible absorption spectra of receptors **L1**, **L2** and complex **L2-F⁻** in chloroform solvent using B3LYP/6-31+G** level theory.

Table S1. Crystal data and structural refinement of receptor L2 .	
CCDC number	1562020
Empirical formula	C ₂₅ H ₂₆ B Fe N O ₂
Formula weight	439.13
Temperature	296(2) K
Wavelength	0.71073 Å
Crystal system, space group	Monoclinic, P21/n
Unit cell dimensions	a = 6.6968(3) Å α = 90° b = 28.3884(15) Å β = 93.970(2)° c = 11.8736(6) Å γ = 90°
Volume	2251.89(19) Å ³
Z, Calculated density	4, 1.295 Mg/m ³
Absorption coefficient	0.690 mm ⁻¹
F(000)	920
Crystal size	0.60 x 0.30 x 0.20 mm
Theta range for data collection	1.43 to 28.25 deg.
Limiting indices	8<=h<=8, -35<=k<=37, -15<=l<=15
Reflections collected / unique	17467 / 5333 [R(int) = 0.0309]
Completeness to theta = 28.25	96.1 %
Absorption correction	Semi-empirical from equivalents
Max. and min. transmission	0.8743 and 0.6822
Refinement method	Full-matrix least-squares on F ²
Data / restraints / parameters	5333 / 0 / 275
Goodness-of-fit on F ²	1.066
Final R indices [I>2sigma(I)]	R1 = 0.0482, wR2 = 0.1072
R indices (all data)	R1 = 0.0695, wR2 = 0.1192
Largest diff. peak and hole	0.384 and -0.530 e. Å ⁻³

Table S2. The selected bond lengths (Å) and bond angles (°) of receptor L2 .	
Atoms	Receptor L2
Average Fe–C	2.0355 (5)
Fe–Cent(1)	2.0338 (5)
Fe–Cent(2)	2.0372 (5)
C(7)–C(11)	1.452 (3)
C(16)–B(1)	1.555 (4)
O(1)–B(1)	1.355 (4)
O(2)–B(1)	1.332 (4)
C(19)–O(1)	1.444 (3)
C(20)–O(2)	1.461 (3)
C(25)–N(1)	1.135 (4)
C(12)–C(25)	1.432 (4)
C(11)–C(7)–Fe(1)	120.01(18)
N(1)–C(25)–C(12)	179.0 (3)
B(1)–O(1)–C(19)	108.9 (2)
B(1)–O(2)–C(20)	108.7 (2)
O(2)–B(1)–O(1)	113.2 (2)
O(2)–B(1)–C(16)	125.1 (3)
O(1)–B(1)–C(16)	121.5 (3)

Table S3. Solvatochromic data [$\tilde{\nu}_{\max}$ (cm^{-1}) of the charge transfer band] for receptors **L1** and **L2** in different solvents with α , β , π^* values by Kamlet and Taft.

Solvents	α	β	π^*	UV-visible ($\Delta\tilde{\nu}_{\max}$)	
				(1)	(2)
DEE	0.27	0.00	0.47	34.84	30.48
DCM	0.13	0.10	0.82	34.84	30.12
CHCl_3	0.20	0.10	0.58	34.72	30.12
EtOAc	0.55	0.00	0.45	34.97	30.48
THF	0.83	0.75	0.62	34.48	30.21
MeOH	1.00	0.66	0.69	34.84	30.30
EtOH	0.54	0.83	0.77	34.84	30.21
ACN	0.35	0.4	0.75	34.84	30.21
DMF	0.88	0.00	0.69	34.48	30.03
DMSO	0.00	0.76	1.00	34.60	29.32

Table S4. Cyclic voltammetry data (potentials vs. FcH/FcH^+), scan rate 100 mVs^{-1} at the glassy carbon electrode of 0.5 mmolL^{-1} solution of ferrocene and receptors **1** and **2** in dry chloroform with 0.1 molL^{-1} of $\text{nBu}_4\text{NClO}_4$ as the supporting electrolyte at $25 \text{ }^\circ\text{C}$.

Compound	E_{pa} (mV)	E_{pc} (mV)	$i_{\text{pc}}/i_{\text{pa}}$ (mV)	$E_{1/2}$ (mV)	ΔE (mV)
Ferrocene	509	438	0.98	473	71
L1	899	823	0.47	861	76
L2	763	693	0.65	728	70

Table S5. Optimized structure of receptors **L1**, **L2** and complex **L2-F** using B3LYP/6-31+G** level of theory.

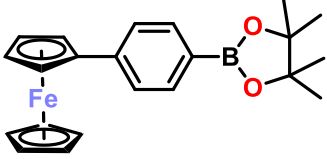
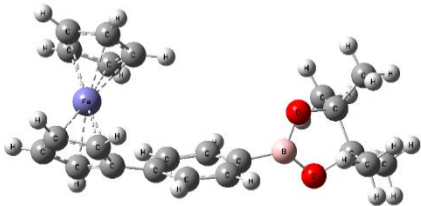
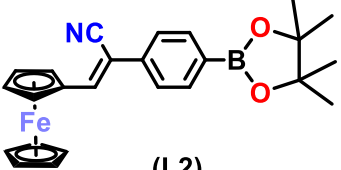
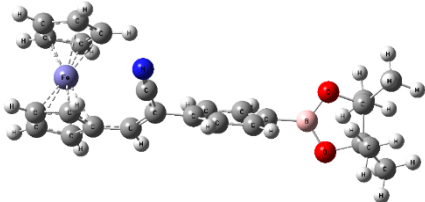
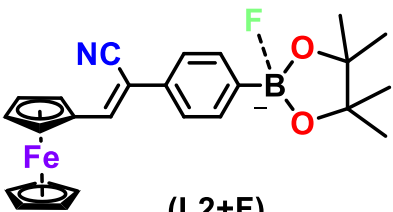
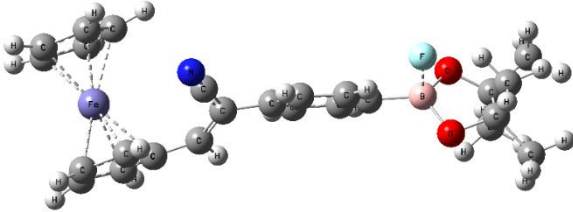
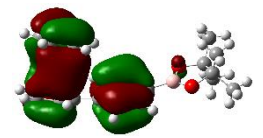
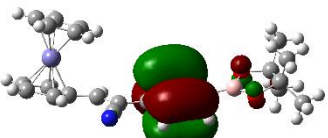
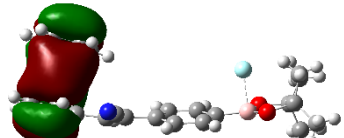
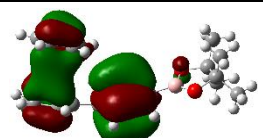
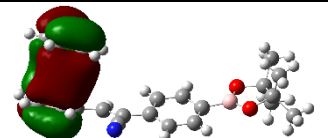
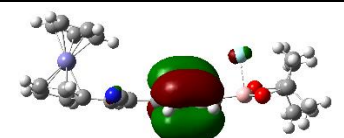
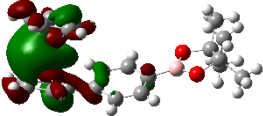
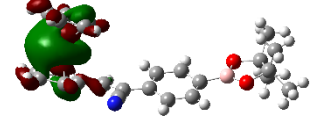
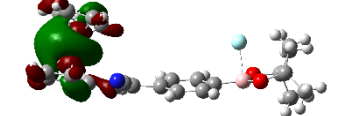
S. No	Compounds	Optimized Structure
1	 <p>(L1)</p>	
2	 <p>(L2)</p>	
3	 <p>(L2+F)</p>	

Table S6. Selected transitions obtained from TD-DFT calculation with B3LYP/6-31+G** level theory using isosurface value of 0.02 au.

S. No	λ_{\max} (nm)	Oscillation strength, <i>f</i>	Energy (eV)	Selected major contributions
Receptor-L1	351	0.0308	3.53	H-3→L+2 (30%)
	310	0.0142	3.99	H-1→L (36%)
	306	0.1301	4.04	H→L (41%)
	280	0.0460	4.43	H→L+1 (59%)
	276	0.2276	4.48	H-2→L (48%)
	273	0.1221	4.55	H-1→L+1 (62%)
	265	0.0102	4.68	H→L+3 (61%)
	260	0.0254	4.77	H-2→L (51%)
	255	0.0214	4.86	H-2→L+2 (60%)
	251	0.0329	4.93	H-4→L (40%), H-2→L+1 (35%),
	249	0.0520	4.99	H-1→L+5 (47%)
	243	0.0142	5.10	H-5→L (53%)

	242	0.0145	5.13	H→L+6 (78%)
Receptor -L2	549	0.0184	2.26	H-1→L (47%)
	532	0.0284	2.33	H-1→L (31%)
	471	0.0691	2.63	H-1→L+3 (33%)
	394	0.0537	3.15	H-1→L+3 (33%), H→L (37%)
	344	0.5240	3.60	H-2→L (30%)
	330	0.3289	3.76	H-3→L+3 (58%)
	284	0.0970	4.36	H-4→L (96%)
	282	0.0302	4.39	H-5→L (78%)
	261	0.0412	4.75	H-6→L (60%)
L2+F ⁻	677	0.0012	1.83	H-6→L (68%)
	672	0.0102	1.84	H-1→L+3 (69%)
	642	0.0210	1.93	H→L+3 (63%)
	628	0.0147	1.97	H-5→L (97%)
	554	0.0351	2.23	H-6→L (83%)
	547	0.0013	2.27	H-1→L (41%), H-2→L (43%),
	510	0.0218	2.43	H-3→L+3 (83%)
	493	0.0333	2.51	H-6→L+3 (87%), H-2→L (65%),
	487	0.0341	2.54	H-2→L+1 (44%),

Table S7. Density surfaces of the frontier orbitals involved in electronic transitions of receptors **L1** and **L2** which is derived from B3LYP/6-31+G** level of theory using isosurface value of 0.02 au.

Orbitals	Receptor-L1	Receptor -L2	L2+F
HOMO-5			
HOMO-4			
HOMO-3			

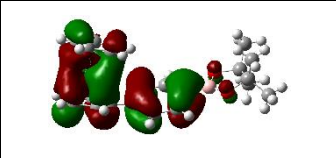
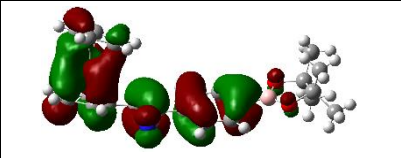
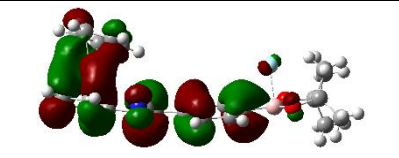
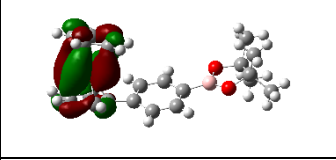
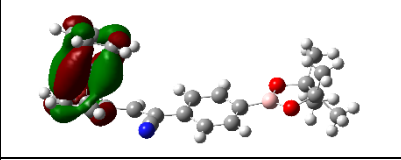
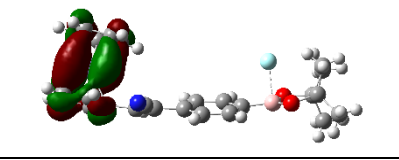
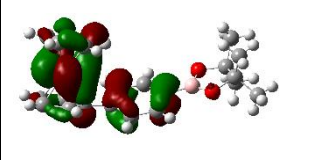
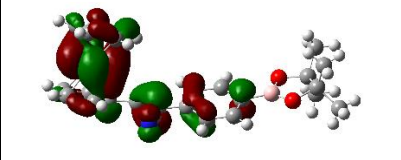
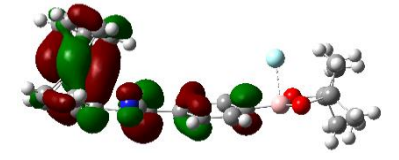
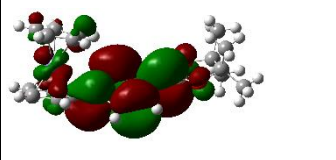
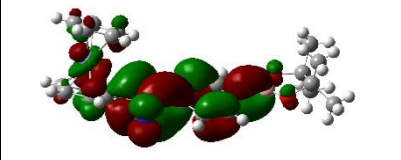
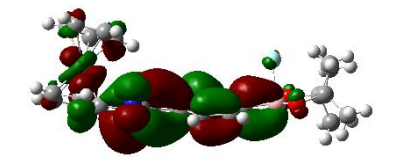
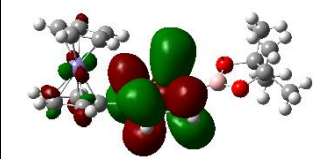
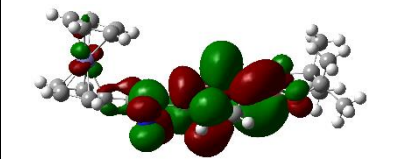
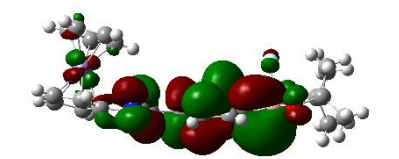
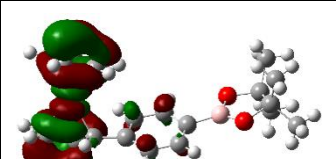
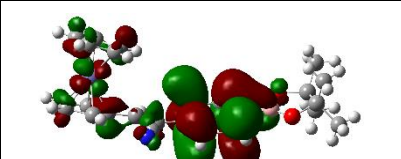
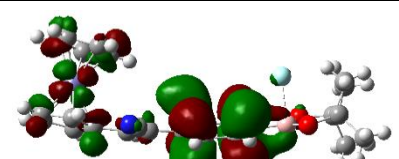
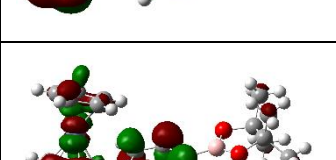

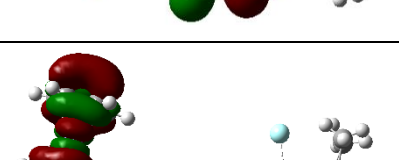
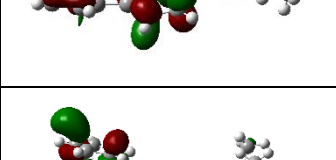
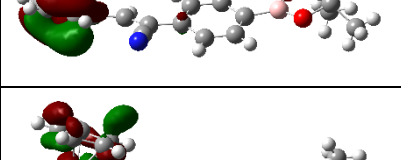
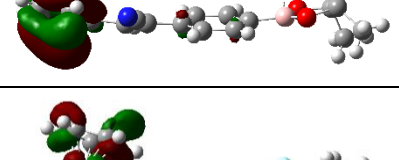
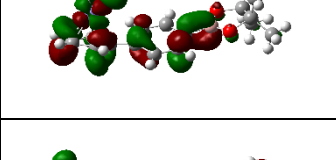
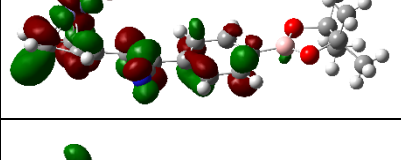
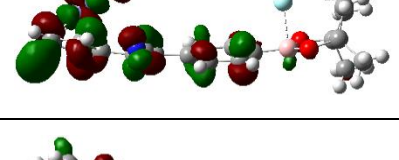
HOMO-2			
HOMO-1			
HOMO			
LUMO			
LUMO+1			
LUMO+2			
LUMO+3			
LUMO+4			
LUMO+5			

Table S8. The computed HOMO and LUMO energy levels, dipole moment and second-order nonlinear optical parameters of receptors **L1** and **L2**.

Receptors	^a E _{HOMO} (eV)	^a E _{LUMO} (eV)	^a Energy gap(eV)	^a μ_{total} (Debye)	^b ω	^b α_0 ($\times 10^{-23}$ esu)	^b β_0 ($\times 10^{-31}$ esu)
L1	-5.409	-1.598	3.81	2.21	3.221	25.917	148.977
L2	-5.725	-2.062	3.66	5.25	4.139	31.850	246.430
L2-F⁻	-2.636	-0.271	2.36	5.33	0.893	--	--

^aTheoretically calculated HOMO, LUMO, band gap and dipole moment values from DFT calculations.
^bElectrophilicity index (ω), Polarizability (α_0) and Hyperpolarizability (β_0) using the gas phase at B3LYP/6-31+G** level of theory.

Reference

- (a) J. Heinze, *Angew. Chemie Int. Ed. English*, 1984, **23**, 831–847; (b) R. S. Nicholson, *Anal. Chem.*, 1965, **37**, 1351–1355; (c) H. Takashima, Y. Inagaki, H. Momma, E. Kwon, K. Yamaguchi and W. Setaka, *Organometallics*, 2018, **37**, 1501–1506.
- H. M. N. H. Irving, H. Freiser and T. S. West, *Compendium of analytical nomenclature: definitive rules 1977*, Elsevier, 2017.
- S. K. Kurtz and T. T. Perry, *J. Appl. Phys.*, 1968, **39**, 3798–3813.
- (a) R. G. Parr, L. V. Szentpály and S. Liu, *J. Am. Chem. Soc.*, 1999, **121**, 1922–1924; (b) P. K. Chattaraj, S. Giri and S. Duley, *Chem. Rev.*, 2006, **106**, 2065.
- Robert G. Parr and Weitao Yang, *J. Am. Chem. Soc.*, 1984, **106**, 4049–4050.
- M. Gopalakrishnan, K. Thirumoorthy, N. S. P. Bhuvanesh and N. Palanisami, *RSC Adv.*, 2016, **6**, 55698–55709.
- H. Saeidian and M. Sahandi, *J. Mol. Struct.*, 2015, **1100**, 486–495.
- R. T. Lynch, M. D. Levenson and N. Bloembergen, *Phys. Lett. A*, 1974, **50**, 61–62.
- (a) P. K. Chattaraj, U. Sarkar and D. R. Roy, *Chem. Rev.*, 2006, **106**, 2065–2091; (b) P. K. Chattaraj, S. Giri and S. Duley, *Chem. Rev.*, 2011, **111**, 43–75.
- R. G. Parr, L. V. Szentpaly and S. Liu, *J. Am. Chem. Soc.*, 1999, **121**, 1922–1924.
- R. G. Parr and W. Yang, *J. Am. Chem. Soc.*, 1984, **106**, 4049–4050.

- 12 H. Saeidian and M. Sahandi, *J. Mol. Struct.*, 2015, **1100**, 486–495.
- 13 R. T. Lynch, M. D. Levenson and N. Bloembergen, *Phys. Lett.*, 1974, **50**, 61–62.
- 14 D. A. Dixion and N. Matsuzawa, *J. Phys. Chem.*, 1994, **98**, 3967–3977.